World J Microbiol Biotechnol (2014) 30:2871–2883
DOI 10.1007/s11274-014-1713-1

ORIGINAL PAPER

Pyruvate decarboxylase and alcohol dehydrogenase overexpression in *Escherichia coli* resulted in high ethanol production and rewired metabolic enzyme networks

Mingfeng Yang · Xuefeng Li · Chunya Bu · Hui Wang · Guanglu Shi · Xiushan Yang · Yong Hu · Xiaoqin Wang

Received: 11 April 2014 / Accepted: 30 July 2014 / Published online: 13 September 2014

Abstract Pyruvate decarboxylase and alcohol dehydrogenase are efficient enzymes for ethanol production in *Zymomonas mobilis*. These two enzymes were overexpressed in *Escherichia coli*, a promising candidate for industrial ethanol production, resulting in high ethanol production in the engineered *E. coli*. To investigate the intracellular changes to the enzyme overexpression for homoethanol production, 2-DE and LC–MS/MS were performed. More than 1,000 protein spots were reproducibly detected in the gel by image analysis. Compared to the wild-type, 99 protein spots showed significant changes in abundance in the recombinant *E. coli*, in which 46 were down-regulated and 53 were up-regulated. Most proteins related to tricarboxylic acid cycle, glycerol metabolism and other energy metabolism were up-regulated, whereas proteins involved in glycolysis and glyoxylate pathway were down-regulated, indicating the rewired metabolism in the engineered *E. coli*. As glycolysis is the main pathway for ethanol production, and it was inhibited significantly in engineered *E. coli*, further efforts should be directed at minimizing the repression of glycolysis to optimize metabolism network for higher yields of ethanol production.

Mingfeng Yang and Xuefeng Li have contributed equally to this work.

M. Yang · C. Bu · G. Shi · X. Wang (✉)
Key Laboratory of Urban Agriculture (North) Ministry of Agriculture, Beijing University of Agriculture, Beijing 102206, China
e-mail: wxqtycn@gmail.com

X. Li · H. Wang · X. Yang · Y. Hu (✉) · X. Wang
College of Life Sciences, Capital Normal University, Beijing 100048, China
e-mail: hybrave@163.com

Keywords *Escherichia coli* · Pyruvate decarboxylase · Alcohol dehydrogenase · Ethanol · Proteomics

Introduction

As the global demand for energy continues to rise and the negative environmental impact of reliance on fossil fuels intensify, biofuels derived from renewable sources have become increasingly important as a clean alternative energy source. A promising renewable resource for biofuel production is lignocellulosic biomass such as straw, bagasse and forestry residues, due to its low cost, widespread abundance. The hydrolysate of lignocellulosics contains both hexose and pentose sugars, such as glucose, galactose, mannose, xylose, and arabinose. By microbial fermentation, all of these sugars can be potentially converted to ethanol, which is a leading biofuel widely pursued in industry.

However, a major challenge for the cost-effective biofuel production is the lack of natural microorganisms that ferment both hexose and pentose sugars into ethanol with high yield. Naturally ethanologenic organisms such as *Saccharomyces cerevisiae* and *Zymomonas mobilis* are potentially useful ethanol producers as they are homoethanol fermenters, but they are limited in their ability to utilize pentose sugars (Jarboe et al. 2007), which constitute up to 90 % of the monomers in hemicellulose (Ingram et al. 1999). *Escherichia coli*, in contrast, can metabolize a wide range of sugars (including pentoses and hexoses), an important feature in obtaining economical yields from lignocellulose hydrolysates (Ingram et al. 1999), but it lacks the native ability for homoethanol production, leading to its poor efficiency in converting pyruvate to ethanol, and only about 10 % ethanol in its fermentation product

(Abanoz et al. 2012). To develop microorganisms capable of fermenting both hexose and pentose sugars in a homoethanol production pathway, either a pentose sugar catabolic pathway is engineered into homoethanol-producing hosts, or a homoethanol pathway is cloned into pentose-fermenting hosts, as did in several micro-organisms such as *Z. mobilis*, *E. coli*, *Klebsiella oxytoca*, and Saccharomyces yeast (Ingram et al. 1987; Beall et al. 1991; Ho et al. 1998; Krishnan et al. 2000; Dien et al. 2003; Yomano et al. 2008).

Zymomonas mobilis is one of the best ethanol producers which produce ethanol in the Entner–Doudoroff (ED) pathway, that is, homoethanol fermentation pathway with the help of two essential enzymes, pyruvate decarboxylase (PDC) and alcohol dehydrogenase (ADH) (Conway 1992). PDC catalyzes the decarboxylation of pyruvate to produce acetaldehyde and carbon dioxide, and then ADH catalyzes the reduction of acetaldehyde to ethanol (Neale et al. 1987; Conway et al. 1987a, b). PDC and ADH are sufficient to convert intracellular pool of pyruvate and NADH to ethanol, and their genes (*pdc* and *adh*) have been usually assembled as the Production of Ethanol (PET) operon (Alterthum and Ingram 1989) and engineered into micro-organisms heterologously expressing the homoethanol pathway from *Z. mobilis*. Some studies used plasmid-based expression of the homoethanol pathway (Alterthum and Ingram 1989; Dien et al. 2000) and others tried chromosomal integration of the heterologous ethanol production cassette, providing greater genetic stability over time (Ohta et al. 1991; Yomano et al. 2008). PET operon has been introduced to *E. coli* for the production of ethanol at rather higher efficiency (Ingram et al. 1987; Lawford and Rousseau 1991; Ohta et al. 1991; Dien et al. 2000; Yomano et al. 2008), but still cannot produce large amounts of ethanol (Dumsday et al. 1999). Similarly, recombinant bacteria, namely *Enterobacter cloacae* JV, *Proteus mirabilis* JV and *Erwinia chrysanthemi* were developed to improve the ethanol production (Piriya et al. 2012). The PET operon has also been introduced into the Gram positive bacteria, *Bacillus subtilis* (Barbosa and Ingram 1994), *Lactobacillus casei* (Gold et al. 1996), and several other lactic acid bacteria (Nichols et al. 2003), but little ethanol was produced.

The primary metabolism of industrial micro-organisms has been studied for long time and most biochemical pathways and reaction networks have been elucidated. In the light of the information, metabolic engineering is used for the introduction of new cellular processes in micro-organisms for industrial production. However, the redirection of metabolic pathways and the rebuilt homeostasis remain elusive in the genetically engineered micro-organism. A better understanding of the complex biochemical network in genetically engineered micro-organisms can help us optimize the industrial fermentation and metabolic pathway. The cell metabolism is a complex network of biochemical reactions that are involved in a large number of metabolites and enzymes (Schuster et al. 2000). Proteome analysis allows profiling of a large number of proteins, which can be used to obtain a global overview of metabolic pathways in engineered micro-organism, and gain a better understanding of flux control and consequently lead to define target enzymes/proteins for further manipulation.

In this work, proteomics was used to examine the protein profiles of *E. coli* containing a recombinant plasmid encoding the pyruvate decarboxylase and alcohol dehydrogenase genes from *Z. mobilis*. The results showed that the introduction of the homoethanol pathway led to global changes of many cellular metabolic pathways including negative effect on glycolysis, indicating that genetically modified *E. coli* need further optimization for high yields of ethanol production.

Materials and methods

Plasmid constructions and bacterial strains

The primers were designed using Primer Premier software (Version5.0, PREMIER Biosoft Inc.) with default parameters to amplify a 1.8 kilobase fragment of pyruvate decarboxylase (*pdc*) gene including its promoter (Conway et al. 1987a) and a 1.3 kilobase fragment of alcohol dehydrogenase (*adhB*) gene including its terminator (Conway et al. 1987b). The primers for promoter and ORF of *pdc* gene were: forward primer, atggatcccactttagaggtttctgggtcat, and reverse primer, gagaattcaaaactagaggagcttgttaacag; the primers for gene of *adhB* with its terminator were: forward primer, gcgtcgactatgtagggtgaggttatagct, and reverse primer, gtagagctcggcaaattatttatgacggta. The fragments amplified by PCR were cloned into pGEM-T vector (Promega, USA) separately, resulting in two recombinant vectors named pGEM-*pdc* and pGEM-*adhB*. The 1.2-kilobase *Sal*I-*Sac*I fragment containing *adhB* was cut from pGEM-*adhB* and inserted into the *Sal*I-*Sac*I site of pGEM-*pdc* to produce pLPA102. Standard transformation procedure was used to introduce pLPA102 into *E. coli* TOP 10. *E. coli* (pLPA102) was grown in LB broth containing 2 % glucose and ampicillin (50 μg/mL) at 37 °C. Bacterial strains and plasmids used in this study are summarized in Table 1.

Fermentation experiments

The recombinant *E. coli* (pLPA102) was grown without antibiotics through all fermentation experiments. In order to prepare the inoculum, a 250 mL volumetric flask containing 100 mL medium was inoculated from a fresh agar

Table 1 Strains and plasmids used in this study

Strain or plasmid	Size (kb)	Relevant genotype, mode of construction, or feature	Reference or source
Strains			
Escherichia coli TOP 10		*F-mcrA Δ(mrr-hsdRMS-mcrBC) φ80lacZΔM15 ΔlacX74 deoR nupG recA1 araD139 Δ(ara-leu)7697 galU galK rpsL(Str^R) endA1 λ$^-$*	Laboratory stock
Zymomonas mobilis CICC 10225		Wild-type strain	Laboratory stock
Plasmids			
pGEM-T	3.0	*T7*; MCS; *SP6*; *lacZα*	Promega
pGEM-*pdc*		Contained promoter and ORF of *pdc* gene	This study
pGEM-*adhB*		Contained ORF of *adhB* gene and its terminator	This study
pLPA102	5.9	pGEM with *pdc* as *Eco*RI-*Eco*RI fragment and *adhB* as *Sal*I-*Sac*I fragment	This study

slant. The inoculum for fermentations was grown overnight in LB broth containing 20 g/L glucose at 37 °C in a rotary shaker at 120 rpm. Fermentation experiments were started with an inoculum initial absorbance 0.3 OD at 550 nm. Fermentations were conducted in 250-mL flasks, which contained LB broth and 50 g/L sugar(s) in 200 mL final volume at 37 °C in a rotatory shaker at 80 rpm. Each flask was sealed with 0.2 μm polyvinylidene fluoride (PVDF) film. Sugar(s) were filter-sterilized as concentrates and added directly to fermentation broth. The pH was maintained at 7.0 by adding of 5 M NaOH. Samples were removed every 4 h during fermentations for the measurement of ethanol production and sugar consumption. The experiment was repeated four times for each sugar, with each experiment started from independent inocula.

The filtered samples were analyzed by gas chromatography equipped with a chromosorb 105 column and a flame ionization detector for ethanol concentration. The maximum theoretical yield of ethanol from sugar is 0.51 g ethanol/g sugar. The ethanol yield (g ethanol/g sugar) was calculated as the maximum concentration of ethanol produced and divided by the starting concentration of sugar.

Growth curve of *E. coli*

The recombinant *E. coli* (pLPA102) and wild type *E. coli* cells were cultured on an LB agar plate at 37 °C for 16 h. Cells from several well-grown colonies were then transferred to a 5 ml of LB broth with shaking (120 rpm) at 37 °C for 12 h. When the absorbance was about 0.3 OD at 550 nm, the same initial inoculum size of both *E. coli* cells (2 μL of *E. coli* cells) were inoculated in 500 mL volumetric flasks containing 300 mL LB broth at 37 °C in a rotatory shaker at 120 rpm. The culture of *E. coli* was sampled at hourly intervals from 2 h incubation through a 20 h incubation period. A graph of OD550 versus Time was plotted to estimate the growth phase of the culture. All the LB medium used above for the recombinant *E. coli* (pLPA102) contained 50 μg/mL ampicillin.

Protein extraction and 2-DE

The recombinant *E. coli* (pLPA102) and wild type *E. coli* were grown in LB broth (with 50 μg/mL ampicillin for the recombinant *E. coli*) at 37 °C in a rotary shaker at 120 rpm. *E. coli* cells were harvested for protein extraction after 12 h of cultivation when the absorbance was about 0.5–0.6 OD at 550 nm. Proteins were extracted using a phenol extraction procedure (Wang et al. 2009). The resulting pellets were dissolved in a sample buffer (7 M urea, 2 M thiourea, 4 % (w/v) CHAPS, 0.5 % (v/v) IPG buffer, 1 % (w/v) DTT) at room temperature. 2-D electrophoresis was carried out according to Bjellqvist et al. (Bjellqvist et al. 1982). Dry IPG strips (18 cm long, pH 4–7 linear) were rehydrated for 12 h in 350 μL rehydration buffer containing 800 μg protein samples. The first dimension separation was conducted at 20 °C with an Ettan IPGphor system (GE Healthcare BIO-Science). Focusing was performed in four steps: 300 V for 1 h, 600 V for 1 h, 1,000 V for 1 h, and 8,000 V for 10 h. Focused strips were then equilibrated by first incubating them in an equilibration solution (6 M urea, 30 % v/v glycerol, 2 % w/v SDS, 50 mM Tris–HCl, pH 8.8, and 1 % w/v DTT) for 15 min, followed by incubation in 4 % w/v iodoacetamide in the same equilibration solution for 15 min. For the second dimension, the proteins were separated on 15 % SDS polyacrylamide gels. Gels were stained with 0.1 % Coomassie brilliant blue (CBB) R-250 in 25 % ethanol/8 % acetic acid and destained in 25 % ethanol/8 % acetic acid. There were three independent biological replicates of each strain in this experiment.

Image and data analysis

The 2-DE gels were scanned at 600 dots per inch (dpi) resolution with a scanner (UMAX Power Look 2100XL, Maxium Tech, Taibei, China). The 2-DE gels were analyzed using the ImageMaster 2D platinum software version 5.0 (GE Healthcare BIO-Science). Spot detection parameters were set as follows: saliency 2.0, partial threshold 4,

and minimum area 50. To verify the auto detected results, all spots were manually inspected. Spot matching between the gels was about 75 % for the different strains (three independent biological replicates in two strains, TOP10 with and without pLPA102) and approximately 85 % of the same strain (three independent biological replicates). After spot detection, quantification, and background subtraction, each analyzed gel was matched individually to the reference gel. To compensate for subtle differences in sample loading, gel staining, and destaining, the volume of each spot (i.e. spot abundance) was normalized as a relative volume. Only those with quantitative changes at least 1.5-fold in abundance (*t* test $P < 0.05$) and reproducible changes among three replicates were used for further analysis.

In-gel digestion and protein identification

Protein spots were manually excised from the gel and in-gel digestion by trypsin was performed according to Wang et al. (Wang et al. 2009). Proteins were identified by LC–MS/MS. A Micromass CapLC quadrupole time-of-flight QTOF2 system (Waters, Milford, MA, USA) consisting of a CapLC, an auto sampler, and a QTOF2 mass spectrometer was used. The mobile phase flow from the C pump was used to preconcentrate and desalt the digest samples on a 5 mm × 300 μm Symmetry C18 precolumn (Waters) for 5 min at 20 μL/min with an aqueous 0.1 % formic acid solution. The Q-TOF spectrometer data were recorded for 1 s on the mass range 400–1,500 *m/z* using the Masslynx software (Waters), after which the two most intense ions were selected and fragmented in the collision cell. The collision energy profiles were optimized for various mass ranges and charge states of precursor ions. Mass data were processed with Protein Lynx Global Server software (Micromass/Waters). Protein identification was achieved by confronting mass data against a nonredundant database (National Center for Biotechnology Information) using the Mascot MS/MS Ions Search algorithm (http://www.matrixscience.com). The searches were performed with tryptic specificity allowing one missed cleavages and the parent ion *m/z* tolerances of 150 ppm and fragment ion *m/z* tolerances of 0.3 Da. All identified peptides were calculated and filtered by 1.0 % false-positive rate (FPR) (Elias and Gygi 2007).

Results and discussion

Plasmid construction

A recombinant plasmid pLPA102 was constructed by insertion of *pdc* and *adhB* genes from *Z. mobilis* into pGEM-T (Fig. 1). The plasmid pLPA102 contains the native *pdc* promoter and the ORF of *pdc*, followed by the gene *adhB* which includes a ribosome-binding site located at 8 bp upstream from the start codon and a 13-bp palindrome which resembles a prokaryotic terminator located 50 bp downstream from the stop codon. Thus, *pdc* and *adhB* were assembled like a 'PET operon', and the expression of the two genes is under the control of *pdc* promoter and *adhB* terminator, which has been shown to be working well in engineering *E. coli* for the production of ethanol (Ingram et al. 1987; Lawford and Rousseau 1991; Dien et al. 2000). In pLPA102, all inserted genes were in the opposite orientation of the *lac* promoter, so induction of the *lac* promoter should not result in the expression of *pdc* or *adhB*. *E. coli* strain TOP10 was transformed with plasmid pLPA102, and the resulted *E. coli* TOP10 containing plasmid pLPA102 was selected for further study.

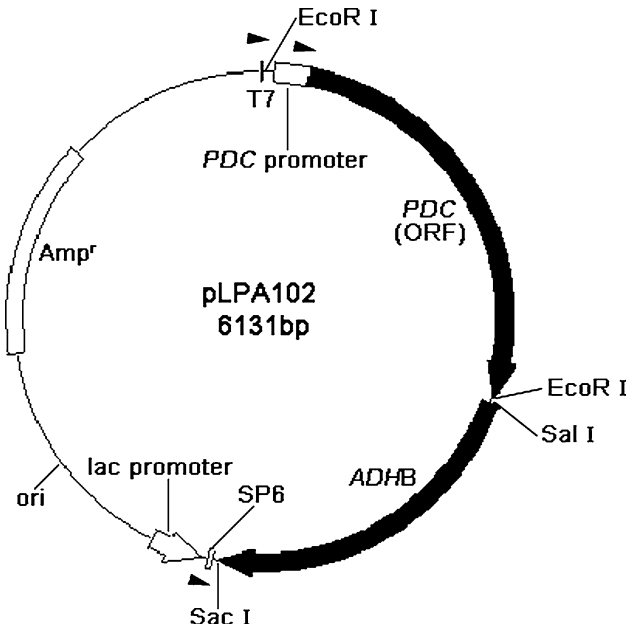

Fig. 1 Physical map of pLPA102

Ethanol production during the fermentation of engineered strains

The recombinant *E. coli* (pLPA102) was grown in broth containing different sugars for fermentation experiments as described in the Materials and methods section, and the ethanol production was calculated (Fig. 2). In the fermentation medium containing 5 % glucose, maximum ethanol concentration was 2.81 % (% vol) (after 40 h), and ethanol yield was 0.449 g ethanol/g sugar for fermentation, which is 88 % of the theoretical maximum (0.51 g ethanol/g sugar). In fermentation medium containing 5 % xylose, maximum ethanol concentration was 2.11 % (after 72 h).

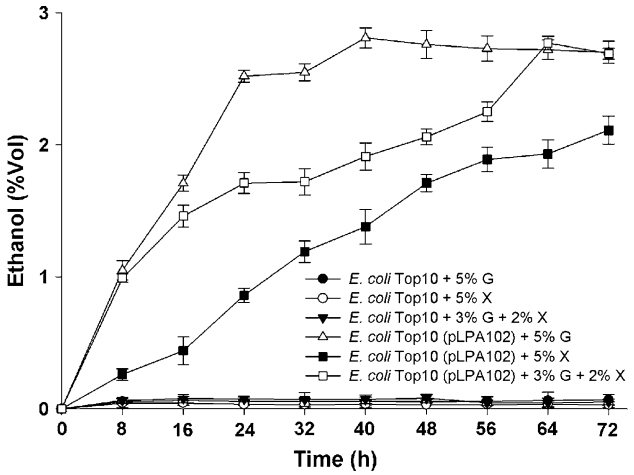

Fig. 2 Ethanol production from 5 % sugar by *E. coli* and *E. coli* (pLPA102). Fermentations were conducted in 250-mL flasks, which contained LB broth and 50 g/L sugar(s) in 200 mL final volume at 37 °C in a rotatory shaker at 80 rpm. Data are presented as means + SD (n = 4). G, glucose; X, xylose

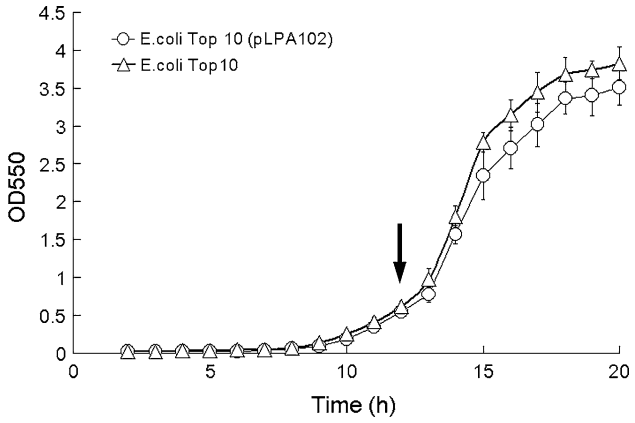

Fig. 3 Growth curve of *E. coli* and *E. coli* (pLPA102). Cells were sampled for proteins extraction (proteomics analysis) after 12 h of cultivation indicated by an *arrow*. Data are presented as means + SD (n = 3)

In sugar mixtures (3 % glucose and 2 % xylose) medium, maximum ethanol concentration was 2.77 % (after 64 h). The results showed that the maximum ethanol concentration for the mixture (glucose plus xylose) was nearly equal to that of glucose, and the maximum ethanol concentration from xylose was lower. In contrast, the maximum ethanol concentration was only 0.07 % for wildtype *E. coli* in the aforementioned mediums, indicating that it could not efficiently utilize xylose and glucose, and produce ethanol at low yields. It showed that the ethanol production of the genetically engineered *E. coli* was significantly improved, and it could efficiently utilize xylose and/or glucose. However, the ethanol yield of the engineered *E. coli* was 88 % of the theoretical maximum, leaving much room of improvement for more ethanol production. Thus, the changes of biochemical network in *E. coli* (pLPA102) were investigated by proteomics to understand the re-established metabolic homeostasis.

Proteins differentially expressed in engineered *E. coli* (pLPA102)

To explore the proteome changes between control and recombinant *E. coli*, comparative proteome investigation has been carried out. In order to keep the recombinant *E. coli* (pLPA102) and wild type *E. coli* in a similar growth condition, both were grown in regular LB broth without adding extra sugar for intense fermentation. After 12 h of cultivation, *E. coli* was harvested for protein extraction when the absorbance was 0.5–0.6 OD at 550 nm. At this period, both recombinant and wild type *E. coli* were still in the exponential growth phase (Fig. 3), indicating the nutrients availability or ethanol was not a limitation factor for the growth. After CBB R-250 staining, more than 1,000 protein spots were reproducibly detected. Comparative analysis showed that there were 115 differentially displayed protein spots whose abundance altered at least 1.5-fold relative to the wildtype control. Of these, 99 were identified (Table 2). Among these identified protein spots, 46 spots represented down-regulated proteins (spots D1–D46; Table 2; Fig. 4), and 53 spots represented up-regulated proteins (spots U1–U53; Table 2; Fig. 4) including four proteins that were induced *de novo* by the recombinant *E. coli* (U13, U51, U52, U53). Quantitative analysis indicated that the abundance of these proteins changed in recombinant *E. coli* (Fig. 5) suggesting that the overexpression of foreign proteins had significant effect on the regulation of native proteins.

The protein spots of interest were excised from 2-D gels. After trypsin autolysis, the digested spots were analyzed by LC–MS/MS. The resulting amino acid sequences were searched against *E. coli* databases using SEQUEST software to identify these proteins (Table 2). The differences between the experimental and theoretical MWs and pIs of some proteins might be attributed to post-translational modification of the proteins.

Except for the unknown category, these differentially expressed proteins could be sorted into ten functional categories (Table 2; Fig. 6) according to their biological function as described in the GO project. These functional classes included energy metabolism (36.4 %), small molecule biosynthesis and degradation (24.2 %), transport (10.1 %), response to stress (6.1 %), translation (5.1 %), response to antibiotic (3.0 %), signal and regulation (2.0 %), proteolysis (2.0 %), transcription (1.0 %) and unknown proteins (10.1 %). In *E. coli* (pLPA102), two enzymes (PDC and ADH) related to ethanol biosynthesis were significantly up-regulated, because these are the enzymes encoded on

Table 2 Differential protein spots identified from engineered *E. coli* (pLPA102) by LC–MS/MS

Metabolic group	Spot no.	Theor./exp. mass (kDa)	Theor./ exp. pI	Accession no.	Description
Energy metabolism (36.4 %)					
Glycolysis (9.1 %)	D6	56.2/57.1	4.96/5.05	gi|161486071	Phosphoglyceromutase
	D13	39.2/47.6	5.35/5.57	gi|190907874	Fructose-bisphosphate aldolase
	D14	39.2/47.8	5.35/5.71	gi|190907874	Fructose-bisphosphate aldolase
	D18	39.5/47.2	6.05/6.24	gi|192926771	Galactose-1-phosphate uridylyl transferase
	D19	39.5/46.3	6.05/6.45	gi|194412248	Galactose-1-phosphate uridylyl transferase
	D23	34.8/42.0	5.35/5.60	gi|110345844	6-phosphofructokinase isozyme I
	D24	33.7/40.3	5.37/5.39	gi|157079547	1-phosphofructokinase
	D29	33.5/41.1	5.99/6.35	gi|157066921	Aldose 1-epimerase family protein
	D37	27.0/35.3	5.57/5.78	gi|26250685	Triosephosphate isomerase
TCA cycle (5.1 %)	D3	66.0/66.9	5.89/6.07	gi|170518101	Fumarate reductase, flavoprotein subunit
	U8	60.3/60.5	6.09/6.47	gi|169889111	Fumarate hydratase (fumarase A), aerobic Class I
	U16	44.0/55.7	5.46/5.53	gi|89107584	Dihydrolipoyltranssuccinase
	U21	39.4/51.2	5.44/6.64	gi|195941230	Type II citrate synthase
	U38	29.6/40.6	6.25/5.13	gi|157835434	Chain A, C123at Mutant Of E. Coli Succinyl-CoA Synthetase Orthorhombic Crystal
Glycerol metabolism (4.0 %)	U7	58.9/63.5	6.18/6.58	gi|218432870	Sn-glycerol-3-phosphate dehydrogenase (anaerobic), large subunit, FAD/NAD(P)-binding
	U15	56.2/53.4	5.20/5.36	gi|218701371	Glycerol kinase
	U29	40.8/48.3	5.31/5.13	gi|218705771	Glycerophospho diester phosphodiesterase
	U35	45.3/46.4	5.55/6.03	gi|117624435	Anaerobic glycerol-3-phosphate dehydrogenase subunit B
Pentose and glucuronate interconversions (5.1 %)	U28	33.9/45.6	4.79/4.78	gi|218556077	Ketodeoxygluconokinase
	U42	27.1/34.5	5.07/5.01	gi|89109625	2-deoxy-D-gluconate 3-dehydrogenase
	U43	27.1/34.2	5.07/5.21	gi|89109625	2-deoxy-D-gluconate 3-dehydrogenase
	U48	26.9/38.9	5.74/5.74	gi|115514219	4-deoxy-L-threo-5-hexosulose-uronate ketol-isomerase
	U49	31.1/38.7	5.67/5.94	gi|169753842	4-deoxy-L-threo-5-hexosulose-uronate ketol-isomerase
Ethanol biosynthesis (3.0 %)	U5	60.9/59.8	5.67/5.78	gi|118391	Pyruvate decarboxylase
	U6	60.9/59.7	5.67/5.91	gi|118391	Pyruvate decarboxylase
	U24	39.3/50.8	5.82/6.28	gi|16128341	Alcohol dehydrogenase class III/glutathione-dependent formaldehyde dehydrogenase
Glucuronate pathway (2.0 %)	D8	60.2/57.8	5.25/5.41	gi|85676766	Malate synthase A
	D10	47.5/52.6	4.99/5.10	gi|110345938	Isocitrate lyase
Pentose phosphate pathway (1.0 %)	D27	35.6/44.1	5.67/6.28	gi|39932377	Transaldolase A
Others (7.1 %)	D35	26.7/33.7	5.24/5.15	gi|117623805	7-alpha-hydroxysteroid dehydrogenase
	U2	72.1/65.2	5.40/5.57	gi|169891359	Acetyl-CoA synthetase
	U11	52.3/55.8	4.88/4.91	gi|26108105	Aldehyde dehydrogenase A
	U12	52.3/55.8	4.88/4.97	gi|191170993	Aldehyde dehydrogenase A
	U13	52.3/54.0	4.94/4.97	gi|188488748	Aldehyde dehydrogenase A
	U17	53.9/53.3	5.33/5.50	gi|193061974	Glucuronate isomerase
	U20	51.6/56.9	6.08/6.56	gi|39932373	Soluble pyridine nucleotide transhydrogenase

Table 2 continued

Metabolic group	Spot no.	Theor./exp. mass (kDa)	Theor./ exp. pI	Accession no.	Description
Small molecule biosynthesis and degradation (24.2 %)					
Purine/pyrimidine nucleotide biosynthesis (7.1 %)	D4	74.4/64.4	5.51/5.91	gi|89108622	Conserved hypothetical protein with nucleoside triphosphate hydrolase domain
	U3	57.3/60.2	5.32/5.58	gi|157163475	Bifunctional phosphoribosylaminoimidazolecarboxamide formyltransferase/IMP cyclohydrolase
	U4	57.3/60.0	5.41/5.68	gi|170518345	Phosphoribosylaminoimidazolecarboxamide formyltransferase/IMP cyclohydrolase
	U10	45.9/53.9	4.73/4.87	gi|209914744	Phosphoribosylglycinamide synthase
	U25	51.5/49.6	5.61/6.23	gi|110342900	Adenylosuccinate lyase
	U32	42.4/49.9	5.26/5.58	gi|218352147	Phosphoribosylglycinamide formyltransferase 2
	U41	27.0/35.5	4.86/4.95	gi|147410	5′-phosphoribosyl-5-aminoimidazole-4-*N*-succinocarboxamide synthetase
Amino acid biosynthesis (7.1 %)	D16	41.7/45.4	5.70/6.04	gi|89107446	Gamma-glutamyl:cysteine ligase
	D20	39.0/47.6	6.07/6.52	gi|110342070	Glutamate 5-kinase
	U18	53.3/52.3	5.82/5.83	gi|130833434	Tryptophanase
	U22	53.4/52.1	5.82/6.32	gi|91074807	Tryptophanase
	U23	45.3/49.6	6.02/6.42	gi|218706054	Serine hydroxymethyltransferase
	U33	40.1/46.9	5.23/5.47	gi|188494031	Glycine cleavage system T protein
	U47	52.7/35.2	5.81/5.48	gi|170519405	Tryptophanase
Other small molecule metabolic process (10.1 %)	D2	68.5/67.7	5.10/5.31	gi|157161078	Beta-D-glucuronidase
	D9	52.6/54.1	5.06/5.34	gi|148533819	Glutamate decarboxylase
	D17	40.7/46.7	5.80/6.19	gi|110344272	1-hydroxy-2-methyl-2-(E)-butenyl 4-diphosphate synthase
	D22	30.6/43.2	5.25/5.55	gi|170081397	NAD synthetase, NH3/glutamine-dependent
	D25	32.6/40.6	5.69/5.75	gi|93115470	dTDP-4-dyhydrorhamnose reductase
	D28	31.6/42.8	5.97/6.53	gi|110344063	Naphthoate synthase
	D30	31.6/40.1	5.86/6.27	gi|89107014	Pantothenate synthetase
	D32	28.1/37.1	5.10/5.16	gi|110341946	3-methyl-2-oxobutanoate hydroxymethyltransferase
	D38	27.2/36.1	5.59/5.96	gi|209918826	3-hydroxy acid dehydrogenase
	U51	23.4/32.6	5.76/6.31	gi|110343377	Riboflavin synthase alpha chain
Transport (10.1 %)	D12	60.3/54.4	6.19/6.00	gi|42475	Dipeptide binding protein (DBP)
	D33	29.0/34.5	6.23/5.11	gi|215265197	Cystine transporter subunit
	D42	18.5/24.3	4.50/4.54	gi|157068490	Bacterioferritin
	U9	48.5/51.6	5.02/4.66	gi|110344139	Long-chain fatty acid transport protein precursor
	U30	43.4/45.6	5.38/5.12	gi|192931382	Maltose/maltodextrin-binding periplasmic protein MalE
	U31	44.1/48.7	5.23/5.40	gi|190902878	Glycine betaine/L-proline ABC transporter, ATP binding
	U37	36.0/42.6	5.88/5.85	gi|115514039	Protein
	U39	33.6/36.9	5.03/4.65	gi|110342264	Glycine betaine transporter subunit
	U52	16.9/22.6	4.95/5.14	gi|12516297	Nucleoside-specific channel-forming protein tsx precursor
	U53	15.8/22.9	5.80/6.17	gi|110345681	Galactitol-specific enzyme IIA of phosphotransferase system High affinity ribose transport protein RbsD

Table 2 continued

Metabolic group	Spot no.	Theor./exp. mass (kDa)	Theor./ exp. pI	Accession no.	Description
Response to stress (6.1 %)	D1	84.1/70.6	5.46/5.68	gi|218558600	Hydroperoxidase II
	D26	31.2/41.0	5.58/5.82	gi|218689960	Chaperone protein HchA
	D34	23.7/33.8	4.86/ 5..09	gi|89107689	Predicted glutathione S-transferase
	D41	18.6/25.3	6.23/5.77	gi|33357155	Chain C DNA protection and binding
	D44	16.1/21.9	4.92/5.09	gi|110345324	Universal stress protein
	D46	16.0/23.1	6.04/6.55	gi|110342431	Putative universal stress protein
Translation (5.1 %)	D5	57.8/61.9	4.97/5.04	gi|110346080	Lysyl-tRNA synthetase, heat inducible
	D11	47.0/54.1	5.55/5.86	gi|2781067	Chain B, Histidyl-tRNA ligase
	U1	87.3/73.7	4.91/5.13	gi|190902117	Histidyl-Adenylate
	U14	52.5/53.2	5.00/5.11	gi|41000	Phenylalanyl-tRNA synthetase, beta-subunit
	U36	36.8/43.4	5.75/6.28	gi|189372029	Asparaginyl-tRNA synthetase
					Phenylalanyl-tRNA synthetase, alpha subunit
Response to antibiotic (3.0 %)	U44	31.6/37.6	5.99/5.31	gi|89077562	Beta-actamase
	U45	29.4/37.3	5.47/5.40	gi|166078578	Beta-lactamase
	U46	31.5/37.1	5.62/5.49	gi|11061109	Penicillin beta-lactamase
	D7	52.7/57.1	4.85/5.26	gi|26106679	Aminoacyl-histidine dipeptidase
	D15	35.5/46.0	5.42/5.49	gi|194413987	Protease 7
Proteolysis (2.0 %)	D36	27.2/33.7	5.60/5.34	gi|49613340	Aerobic respiration control protein
	D43	17.1/24.3	5.18/5.28	gi|157065928	Phosphatidylethanolamine-binding protein
Signal and regulation (2.0 %)	U26	38.0/49.3	4.68/4.79	gi|12517195	RNA polymerase, sigma S (sigma38) factor; synthesis of many growth phase related proteins
Transcription (1.0 %)	D21	35.5/43.6	4.87/5.06	gi|170019580	ADP-ribosylation/crystallin J1
	D31	34.5/38.9	5.83/5.10	gi|145579688	Chain a crystal structure of a disulfide mutant glucose binding protein
Unknown protein (10.1 %)	D39	27.0/36.8	6.15/6.43	gi|12517581	Putative enzyme
	D40	21.1/28.1	6.38/5.38	gi|89111083	Periplasmic protein
	D45	11.3/21.2	5.18/5.48	gi|110344067	Hypothetical protein ElaB (putative membrane protein)
	U19	106.9/55.3	5.80/6.39	gi|7243714	Antigen 43 precursor
	U27	37.0/45.3	4.39/4.29	gi|157831182	Chain A, Ompf Porin (Mutant R132p)
	U34	36.6/44.2	5.13/5.34	gi|110641886	Selenophosphate synthetase
	U40	27.8/35.4	5.41/4.81	gi|188016313	MltA-interacting protein MipA
	U50	22.2/32.8	5.41/5.62	gi|13096116	Chain C, Schiff Base Intermediate In Kdpg Aldolase

All the protein identities were from searching in NCBInr database

D, down-regulated; U, up-regulated; Theor./exp. Mass (kDa), theoretical and experimental molecular mass in kilodaltons; Theor./exp. pI, theoretical and experimental isoelectric point

pLPA102 and expressed in the recombinant strain. The significant changes of the proteomics profile in *E. coli* (pLPA102) indicate the restructured metabolic networks in recombinant strain.

Changes of energy metabolic proteins

Compared to wildtype *E. coli*, 33 proteins categorized within the energy metabolism group were altered dramatically in *E. coli* (pLPA102) (Table 2; Figs. 4, 5, 6a). Among these proteins, 11 were down-regulated and 22 were either induced or up-regulated. Proteins of this category are involved in basic energy metabolism such as glycolysis, tricarboxylic acid (TCA), glycerol metabolism, pentose and glucuronate interconversions, ethanol biosynthesis, glucuronate pathway, glyoxylate cycle and pentose phosphate pathway. Most differentially expressed proteins were categorized in energy metabolism (36.4 %), suggesting that the energy metabolism was altered dramatically in *E. coli* (pLPA102) strain (Fig. 6a).

Glycolysis is the metabolic pathway that converts glucose into pyruvate, where free energy is released to form the high-energy compounds ATP (adenosine triphosphate) and NADH (reducing power). In *E. coli* (pLPA102) strain,

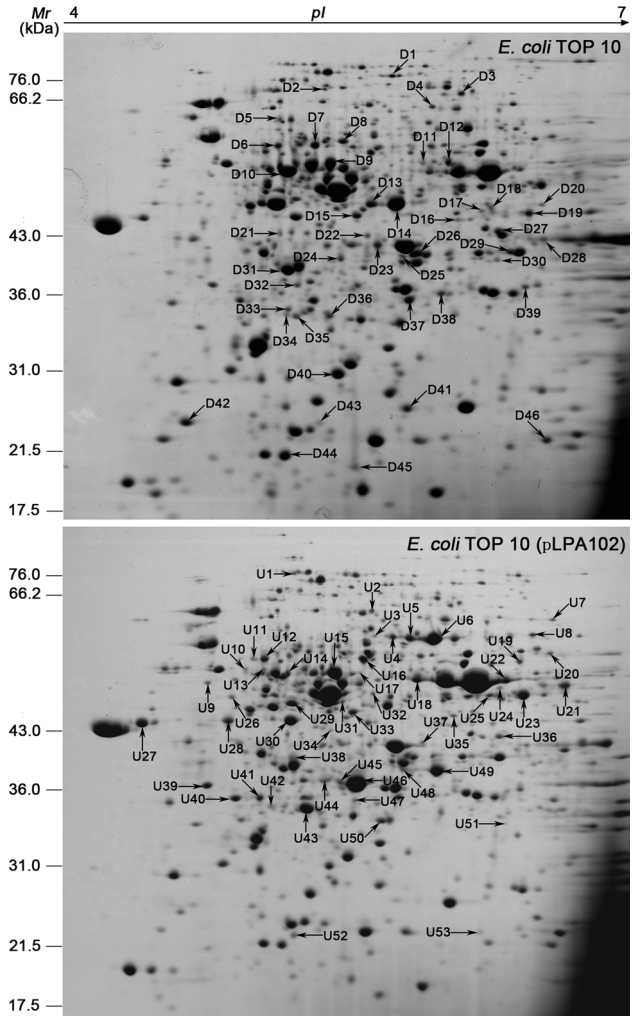

Fig. 4 Proteomics analysis of recombinant *E. coli* expressing *Z. mobilis pdc* and *adh* genes. The recombinant *E. coli* (pLPA102) and wild type *E. coli* were grown in LB broth (with 50 μg/mL ampicillin for the recombinant *E. coli*) at 37 °C in a rotary shaker at 120 rpm. *E. coli* cells were harvested for protein extraction after 12 h of cultivation when the absorbance was about 0.5–0.6 OD at 550 nm. The *arrows* indicate the differential expression proteins. Down-regulated proteins (spots D1–D46) are indicated in the control (*E. coli* TOP 10) image. Up-regulated proteins and newly-induced proteins (spots U1–U53) are indicated in the image of recombinant *E. coli* expressing *Z. mobilis pdc* and *adh* genes [*E. coli* TOP 10 (pLPA102)]

the proteins involved in glycolysis were down-regulated (Fig. 6b). These proteins include phosphoglyceromutase, fructose-bisphosphate aldolase, galactose-1-phosphate uridylyl transferase, which catalyzes the interconversion of UDP-glucose and galactose-1-phosphate with UDP-galactose and glucose-1-phosphate in the reactions of the Leloir pathway of galactose metabolism (Field et al. 1989), phosphofructokinase, aldose 1-epimerase family protein and triosephosphate isomerase. This suggested that glycolysis pathway was inhibited in *E. coli* (pLPA102). Through a metabolite analysis, another study group also found that the glucose metabolism rate was inhibited but the final ethanol yield was slightly increased (Palmqvist et al. 1999), and this was consistent with our study.

The TCA cycle provided the carbon skeletons used in many biosynthetic reactions. Except for fumarate reductase, the proteins related to TCA were up-regulated in *E. coli* (pLPA102) strain. There were fumarate hydratase (fumarase A), dihydrolipoyltranssuccinase, type II citrate synthase and succinyl-CoA Synthetase Orthorhombic Crystal. The inhibition of glycolysis and the increase of ethanol biosynthesis might have resulted in the decrease of acetate-CoA biosynthesis from the pyruvate pathway. However, the down-regulated malate synthase could repress the acetyl-CoA and glyoxlate to synthesize malate, and the up-regulation of acetyl-CoA synthetase could replenish acetyl-CoA into TCA cycle. The increased synthesis acetate-CoA and TCA cycle-related enzymes might have been caused by the cellular effort to overcome the metabolic imbalance in cellular pathways (Kim et al. 2005), and it could enhance the generation of the precursor metabolites and the energy for cell growth.

In the *E. coli* (pLPA102) strain, several proteins involved in glycerol metabolism were found to be up-regulated. Sn-glycerol-3-phosphate (glycerol-P) dehydrogenase, glycerophosphodiester phosphodiesterase (GDPD) and glycerol kinase were related to glycerol catabolism. Glycerol is a three carbon alcohol and it is metabolized quite readily into the dihydroxyacetone phosphate which could be converted into pyruvic acid through the glycolysis pathway to make energy (Murarka et al. 2008). The up-regulation of two enzymes involved in glycerol metabolism suggested that glycerol can be utilized as a source of carbon and energy in *E. coli* (pLPA102) strain, and this is in agreement with previous reports (Murarka et al. 2008). This should be an advantage of engineered *E. coli* for ethanol production, as glycerol is an inexpensive and abundant carbon source. Two proteins involved in pentose and glucuronate interconversions, 2-deoxy-D-gluconate 3-dehydrogenase and 4-deoxy-L-threo-5-hexosulose-uronate ketol-isomerase, were found to be up-regulated, and this might facilitate the use of glucuronate as a source of carbon.

In addition to the aforementioned proteins, two proteins involved in the glyoxylate cycle (malate synthase; isocitrate lyase) and one protein in pentose phosphate pathway (transaldolase) were down-regulated in *E. coli* (pLPA102) strain.

Proteins involved in small molecule biosynthesis and degradation

Six proteins involved in purine and pyrimidine ribonucleotide biosynthesis were sharply up-regulated and one protein was down-regulated. These proteins were phosphoribosylaminoimidazolecarboxamide formyltransferase/IMP cyclohydrolase, phosphoribosylglycinamide

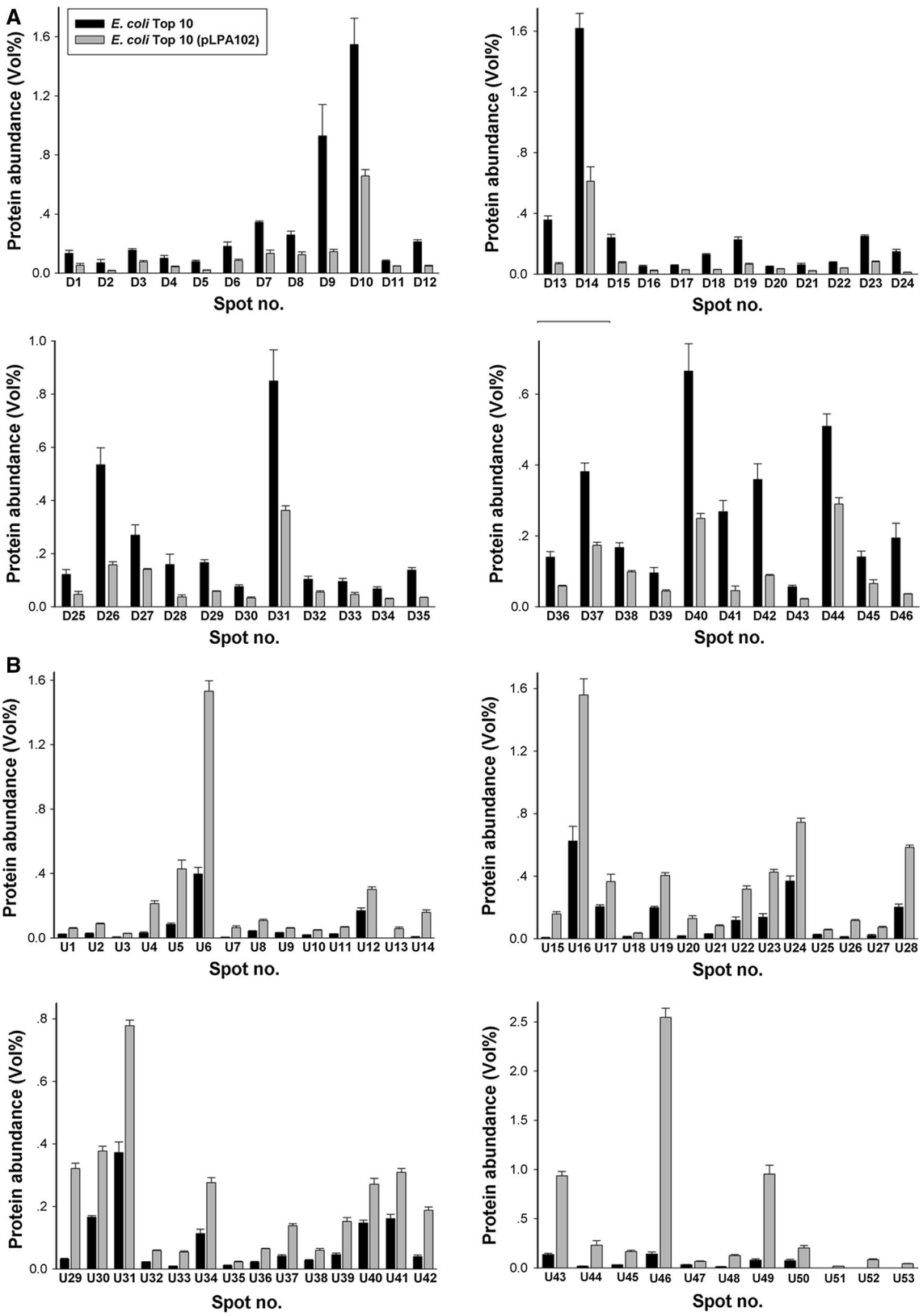
A
E. coli Top 10
E. coli Top 10 (pLPA102)
Protein abundance (Vol%)
Spot no.
D1 D2 D3 D4 D5 D6 D7 D8 D9 D10 D11 D12
D13 D14 D15 D16 D17 D18 D19 D20 D21 D22 D23 D24
D25 D26 D27 D28 D29 D30 D31 D32 D33 D34 D35
D36 D37 D38 D39 D40 D41 D42 D43 D44 D45 D46
B
U1 U2 U3 U4 U5 U6 U7 U8 U9 U10 U11 U12 U13 U14
U15 U16 U17 U18 U19 U20 U21 U22 U23 U24 U25 U26 U27 U28
U29 U30 U31 U32 U33 U34 U35 U36 U37 U38 U39 U40 U41 U42
U43 U44 U45 U46 U47 U48 U49 U50 U51 U52 U53

◀**Fig. 5** Relative abundances (%) of individual different expression proteins. **a** Proteins down-regulated as identified in Fig. 3; **b** Proteins up-regulated as identified in Fig. 3. The protein abundance is presented as the percentage of the total spot volume associated with each identified spot

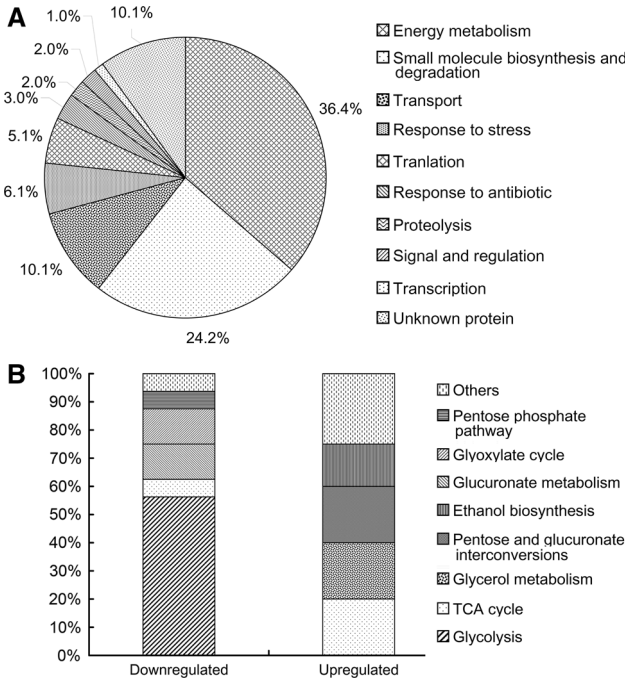

Fig. 6 Functional categorization of the differential expression proteins. **a** Ten functional categories of the identified proteins. **b** Down-regulated and up-regulated proteins

synthase, adenylosuccinate lyase, phosphoribosylglycinamide formyltransferase 2,5′-phosphoribosyl-5-aminoimidazole-4-*N*-succinocarboxamide synthetase, and conserved hypothetical protein with nucleoside triphosphate hydrolase domain.

Differential expressions of proteins involved in amino acid metabolism have also been identified. Tryptophanase, serine hydroxymethyltransferase (SHMT) and glycine cleavage system T protein were up-regulated; Gamma-glutamyl:cysteine ligase (GCL) and glutamate 5-kinase were down-regulated in the *E. coli* (pLPA102) strain.

Several proteins related to other small molecule metabolic processes were also identified. These proteins included riboflavin synthase, glutamate decarboxylase (GAD), NAD synthetase, dTDP-4-dehydrorhamnose reductase, naphthoate synthase, pantothenate synthetase, 3-methyl-2-oxobutanoate hydroxymethyltransferase and 3-hydroxy acid dehydrogenase.

The growth rate dependent regulation of the enzymes involved in pyrimidine, purine nucleotide and amino acid biosynthesis were reported (Raman et al. 2005). The genes up-regulated in the exponential phase equipped cells with enhanced nucleotide biosynthesis and amino acid biosynthesis (Raman et al. 2005). We observed the up-regulation of six enzymes directly involved in the *de novo* synthesis of pyrimidine nucleotide and purine nucleotide biosynthesis. Two amino acid (tryptophan and glycine) biosynthetic enzymes were also up-regulated in *E. coli* (pLPA102) strain. Within many organisms, tryptophan is an essential amino acid during cell growth, participating in nitrogen metabolism (Cowell et al. 1973). The expression of the tryptophan biosynthetic operon was activated by tryptophan depletion and general amino acid starvation (Raya et al. 1998). Glycine is a non-essential amino acid needed to enhance endurance and energy levels (Balsom et al. 1994). *E. coli* is capable of utilizing amino acids as sole sources of carbon and energy (McFall and Newman 1996). The up-regulation of amino acid biosynthetic enzymes might be resulted from the new cellular homeostasis or a part of the tolerance mechanism under an ethanol stress environment as indicated in previous report (Horinouchi et al. 2010).

Changes in transport proteins

The expression levels of ten proteins involved in transport were significantly changed (Table 2; Figs. 4, 5). Seven proteins were up-regulated and three proteins were down-regulated. The up-regulated proteins included long-chain fatty acids transport protein, maltose/maltodextrin-binding periplasmic protein MalE, glycine betaine/L-proline ABC transporter, glycine betaine transporter, nucleoside-specific channel-forming protein tsx precursor, phosphoenolpyruvate (PEP)-dependent phosphotransferase system (PTS) and high affinity ribose transport protein RbsD. Dipeptide binding protein (DBP), cystine transporter and bacterioferritin were down-regulated.

Transport systems play a crucial role for the adaptation of cells to limited resources, because the uptake of a nutrient into the cell is a prerequisite for its utilization. Those proteins upregulated may have played an important role in the transport of nutrients into the cell of the recombinant *E. coli*. The upregulation of several membrane proteins was observed in the *E. coli* (pLPA102) strain. Maltose can be broken down into two glucose molecules by hydrolysis. *E. coli* uses the phospho-transferase system (PTS) for glucose transport during growth on millimolar glucose concentrations (Death and Ferenci 1994). The up-regulation of Maltose/maltodextrin-binding periplasmic protein MalE and the phospho-transferase system (PTS) suggested that the *E. coli* (pLPA102) strain were in glucose starvation and needed to replenish other sugar for energy generation and cell growth. In addition, the up-regulation of long-chain fatty acids transport protein, glycine betaine/L-proline ABC transporter and high affinity ribose transport protein RbsD could provide more metabolites and energy for the growth of the *E. coli* (pLPA102) strain.

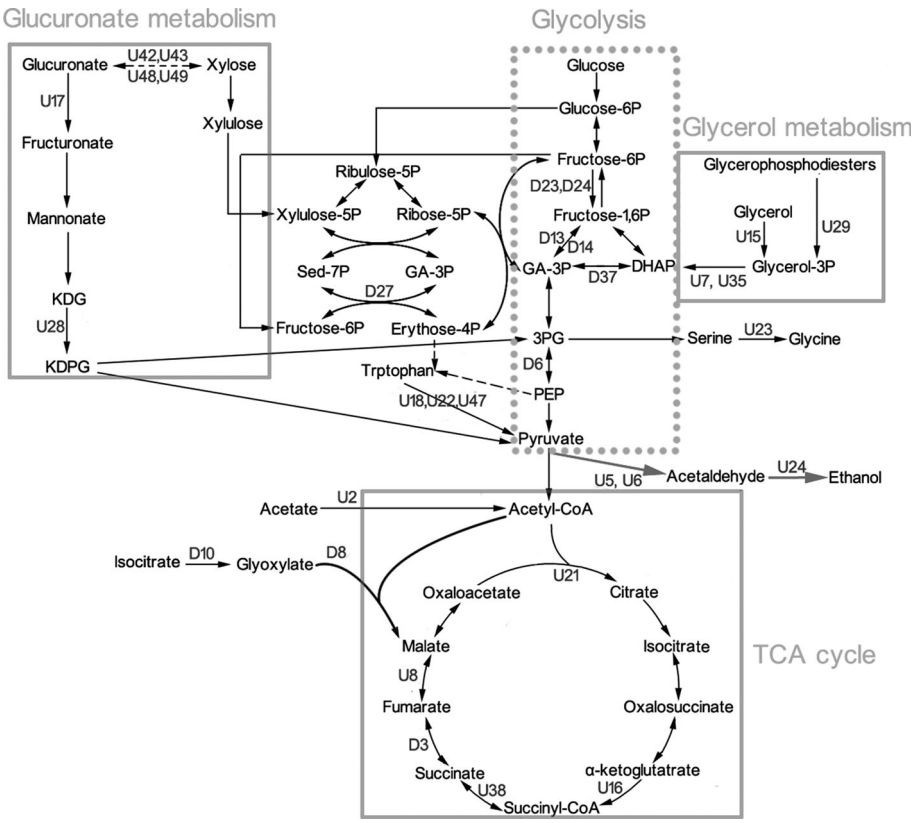

Fig. 7 The rewired network of energy metabolism in *E. coli* (pLPA102) The differential expression proteins involved in energy metabolic pathway, including glycolysis, TCA cycle, glycerol metabolism, glucuronate metabolism, ethanol biosynthesis, glyoxylate cycle, pentose phosphate pathway, and amino acid biosynthesis. Glucuronate metabolism, glycerol metabolism, and TCA cycle, which was upregulated, is highlighted in *solid line box*, and glycolysis, which were downregulated, in *dotted line box*. DHAP, dihydroxyacetone phosphate; GA-3P, glyceraldehyde 3-phosphate; KDG, 2-dehydro-3-deoxy-D-gluconate; KDPG, 2-dehydro-3-deoxy-D-gluconate-6-phosphate; 3PG, 3-phosphoglycerate; PEP, phosphoenolpyruvate; Sed-7P, sedoheptulose 7-phosphate

Profile of the rewired metabolic enzyme networks

Microorganism metabolism is a complex network of chemical reactions that converts sources of energy and chemical elements into biomass and other molecules. In this study, the replacement of the native fermentation pathway in *E. coli* with a homoethanol pathway from *Z. mobilis* (*pdc* and *adhB* genes) resulted in a significant increase in ethanol production during the fermentation of xylose and glucose. The proteomics changes of the engineered *E. coli* (pLPA102) revealed a re-established metabolic network (Fig. 7). Most proteins involved in energy metabolism (except for proteins involved in glycolysis), purine/pyrimidine ribonucleotide biosynthesis, amino acid biosynthesis, and transport were up-regulated, suggesting that in response to a significant up-regulation of foreign proteins, other pathways were readjusted to reach a new balance in cells, and these up-regulated proteins and pathways cooperated in ethanol production efficiently. Except for maintaining metabolic homeostasis, these coordinating changes in proteome might also be used to adapt to new internal and external environments with high ethanol content. As the glycolysis was inhibited significantly when compared with other energy metabolism in the engineered *E. coli* (Figs. 6b, 7), further efforts should been directed at minimizing the repression of glycolysis to improve the metabolism of sugar mixtures for more ethanol production.

The increased abundance of some proteins does not necessarily signify increased in vivo catalytic activity. Nonetheless, these results will underpin the choice of targets for manipulation by metabolic engineers and make metabolic engineering more predictable with less guesswork, decrease the cost of engineering metabolic pathways, and encourage the development of novel solutions to the challenge of engineering efficient ethanologenic microorganisms.

Acknowledgments This work was supported by grants from Beijing Natural Science Foundation (Nos. 5132004, 6122005), National Natural Science Foundation of China (Nos. 30970250, 31370674), China Postdoctoral Science Foundation to Dr. Wang, and Science and Technology Platform Construction Program of Beijing Municipal Commission of Education (PXM2012_014207_000028) and Beijing University of Agriculture (2014).

References

Abanoz K, Stark BC, Akbas MY (2012) Enhancement of ethanol production from potato-processing wastewater by engineering *Escherichia coli* using Vitreoscilla haemoglobin. Lett Appl Microbiol 55:436–443

Alterthum F, Ingram LO (1989) Efficient ethanol production from glucose, lactose, and xylose by recombinant *Escherichia coli*. Appl Environ Microbiol 55:1943–1948

Balsom PD, Soderlund K, Ekblom B (1994) Creatine in humans with special reference to creatine supplementation. Sports Med 18:268–280

Barbosa MS, Ingram LO (1994) Expression of the *Zymomonas mobilis* alcohol dehydrogenase II (adhB) and pyruvate decarboxylase (pdc) genes in Bacillus. Curr Microbiol 28:279–282

Beall DS, Ohta K, Ingram LO (1991) Parametric studies of ethanol production form xylose and other sugars by recombinant *Escherichia coli*. Biotechnol Bioeng 38:296–303

Bjellqvist B, Ek K, Righetti PG, Gianazza E, Gorg A, Westermeier R, Postel W (1982) Isoelectric focusing in immobilized pH gradients: principle, methodology and some applications. J Biochem Biophys Methods 6:317–339

Conway T (1992) The Entner–Doudoroff pathway: history, physiology and molecular biology. FEMS Microbiol Lett 103:1–27

Conway T, Osman YA, Konnan JI, Hoffmann EM, Ingram LO (1987a) Promoter and nucleotide sequences of the *Zymomonas mobilis* pyruvate decarboxylase. J Bacteriol 169:949–954

Conway T, Sewell GW, Osman YA, Ingram LO (1987b) Cloning and sequencing of the alcohol dehydrogenase II gene from *Zymomonas mobilis*. J Bacteriol 169:2591–2597

Cowell JL, Maser K, DeMoss RD (1973) Tryptophanase from *Aeromonas liquifaciens*. Purification, molecular weight and some chemical, catalytic and immunological properties. Biochim Biophys Acta 315:449–463

Death A, Ferenci T (1994) Between feast and famine: endogenous inducer synthesis in the adaptation of *Escherichia coli* to growth with limiting carbohydrates. J Bacteriol 176:5101–5107

Dien B, Nichols N, O'Bryan P, Bothast R (2000) Development of new ethanologenic *Escherichia coli* strains for fermentation of lignocellulosic biomass. Appl Biochem Biotechnol 84–86:181–196

Dien BS, Cotta MA, Jeffries TW (2003) Bacteria engineered for fuel ethanol production: current status. Appl Microbiol Biotechnol 63:258–266

Dumsday GJ, Zhou B, Yaqin W, Stanley GA, Pamment NB (1999) Comparative stability of ethanol production by *Escherichia coli* KO11 in batch and chemostat culture. J Ind Microbiol Biotechnol 23:701–708

Elias JE, Gygi SP (2007) Target-decoy search strategy for increased confidence in large-scale protein identifications by mass spectrometry. Nat Methods 4:207–214

Field TL, Reznikoff WS, Frey PA (1989) Galactose-1-phosphate uridylyltransferase: identification of histidine-164 and histidine-166 as critical residues by site-directed mutagenesis. Biochemistry 28:2094–2099

Gold RS, Meagher MM, Tong S, Hutkins RW, Conway T (1996) Cloning and expression of the *Zymomonas mobilis* "production of ethanol" genes in *Lactobacillus casei*. Curr Microbiol 33:256–260

Ho NWY, Chen Z, Brainard AP (1998) Genetically engineered Saccharomyces yeast capable of effective cofermentation of lucose and xylose. Appl Environ Microbiol 54:1852–1859

Horinouchi T, Tamaoka K, Furusawa C, Ono N, Suzuki S, Hirasawa T, Yomo T, Shimizu H (2010) Transcriptome analysis of parallel-evolved *Escherichia coli* strains under ethanol stress. BMC Genom 11:579

Ingram LO, Conway T, Clark DP, Sewell GW, Preston JF (1987) Genetic engineering of ethanol production in *Escherichia coli*. Appl Environ Microbiol 53:2420–2425

Ingram LO, Aldrich HC, Borges ACC, Causey TB, Martinez A, Morales F (1999) Enteric bacterial catalysts for fuel ethanol production. Biotechnol Prog 15:855–866

Jarboe LR, Grabar TB, Yomano LP, Shanmugan KT, Ingram LO (2007) Development of ethanologenic bacteria. In: Olsson L (ed) Biofuels pp 237–261

Kim YH, Han KY, Lee K, Lee J (2005) Proteome response of *Escherichia coli* fed-batch culture to temperature downshift. Appl Microbiol Biotechnol 68:786–793

Krishnan MS, Blanco M, Shattuck CK, Nghiem NP, Davison BH (2000) Ethanol production from glucose and xylose by immobilized *Zymomonas mobilis* CP4(pZB5). Appl Biochem Biotechnol 84–86:525–541

Lawford HG, Rousseau JD (1991) Ethanol production by recombinant *Escherichia coli* carrying genes from *Zymomonas mobilis*. Appl Biochem Biotechnol 28–29:221–236

McFall E, Newman EB (1996) Amino acids as carbon sources. *Escherichia coli* and Salmonella: Cellular and molecular biology. Washington, DC: ASM Press: 358–379

Murarka A, Dharmadi Y, Yazdani SS, Gonzalez R (2008) Fermentative utilization of glycerol by *Escherichia coli* and its implications for the production of fuels and chemicals. Appl Environ Microbiol 74:1124–1135

Neale AD, Scopes RK, Wettenhall RE, Hoogenraad NJ (1987) Pyruvate decarboxylase of *Zymomonas mobilis*: isolation, properties, and genetic expression in *Escherichia coli*. J Bacteriol 169:1024–1028

Nichols NN, Dien BS, Bothast RJ (2003) Engineering lactic acid bacteria with pyruvate decarboxylase and alcohol dehydrogenase genes for ethanol production from *Zymomonas mobilis*. J Ind Microbiol Biotechnol 30:315–321

Ohta K, Beall DS, Mejia JP, Shanmugam KT, Ingram LO (1991) Genetic improvement of *Escherichia coli* for ethanol production: chromosomal integration of *Zymomonas mobilis* genes encoding pyruvate decarboxylase and alcohol dehydrogenase II. Appl Environ Microbiol 57:893–900

Palmqvist E, Almeida JS, Hahn-Hagerdal B (1999) Influence of furfural on anaerobic glycolytic kinetics of *Saccharomyces cerevisiae* in batch culture. Biotechnol Bioeng 62:447–454

Piriya PS, Vasan PT, Padma VS, Vidhyadevi U, Archana K, Vennison SJ (2012) Cellulosic ethanol production by recombinant cellulolytic bacteria harbouring pdc and adh II genes of *Zymomonas mobilis*. Biotechnol Res Int. doi:10.1155/2012/817549

Raman B, Nandakumar MP, Muthuvijayan V, Marten MR (2005) Proteome analysis to assess physiological changes in *Escherichia coli* grown under glucose-limited fed-batch conditions. Biotechnol Bioeng 92:384–392

Raya R, Bardowski J, Andersen PS, Ehrlich SD, Chopin A (1998) Multiple transcriptional control of the *Lactococcus lactis trp* operon. J Bacteriol 180:3174–3180

Schuster S, Fell DA, Dandekar T (2000) A general definition of metabolic pathways useful for systematic organization and analysis of complex metabolic networks. Nat Biotechnol 18:326–332

Wang XQ, Yang PF, Liu Z, Liu WZ, Hu Y, Chen H, Kuang TY, Pei ZM, Shen SH, He YK (2009) Exploring the mechanism of *Physcomitrella patens* desiccation tolerance through a proteomic strategy. Plant Physiol 149:1739–1750

Yomano LP, York SW, Zhou S, Shanmugam KT, Ingram LO (2008) Re-engineering *Escherichia coli* for ethanol production. Biotechnol Lett 30:2097–2103